REPORT DOCUMENTATION PAGE

AD-A278 352

1. AGENCY USE ONLY (Leave blank)	2. REPORT DATE	3. REPORT TYPE AND DATES COVERED
	03-31-94	Final 01 Sept 93 - 28 Feb 94

4. TITLE AND SUBTITLE
Hardware Implementation of Time Lenses and Ultrafast Optical Temporal Processors

5. FUNDING NUMBERS
C-F49620-93-C-0062

6. AUTHOR(S)
Dr. Xiangyang Yang

7. PERFORMING ORGANIZATION NAME(S) AND ADDRESS(ES)
Quantex Corporation
2 Research Court
Rockville, MD 20850

8. PERFORMING ORGANIZATION REPORT NUMBER
AFOSR-TR- 94 0235
N/A

9. SPONSORING / MONITORING AGENCY NAME(S) AND ADDRESS(ES)
Air Force Office of Scientific Research
110 Duncan Avenue Suite B115
Bolling AFB DC 20332

10. SPONSORING / MONITORING AGENCY REPORT NUMBER
1602 01

11. SUPPLEMENTARY NOTES

12a. DISTRIBUTION / AVAILABILITY STATEMENT
Approved for public release; distribution unlimited.
Unlimited

12b. DISTRIBUTION CODE

13. ABSTRACT *(Maximum 200 words)*

The concept of time lens is based on the analogy between optical spatial diffraction and temporal dispersion. It extends our knowledge of optics in the space-domain into the time-domain. Novel temporal imaging and signal processing systems can be created that mimic the operation of their spatial counterparts in the space-domain. A distinktive advantage of these temporal processing systems is their extremly high speed, up to picosecond range with currently available devices. In this Phase I program, we have studied the space-time duality and established a theoretical model for general temporal imaging systems. Design criteria for a phase chirp modulator as well as dispersive delay lines have been developed. Several temporal imaging and signal processing systems have been designed with commercially available optical and optoelectronic devices. Various applications of these temporal processing systems were studied. A temporal microscope and a temporal 4-f filtering system have been identified for prototype development in Phase II.

14. SUBJECT TERMS	15. NUMBER OF PAGES
Time Lens; Optical Temporal Imaging and Processing Diffraction; Dispersion; Space-Time Duality	29
	16. PRICE CODE

17. SECURITY CLASSIFICATION OF REPORT	18. SECURITY CLASSIFICATION OF THIS PAGE	19. SECURITY CLASSIFICATION OF ABSTRACT	20. LIMITATION OF ABSTRACT
Unclassified	Unclassified	Unclassified	SAR

Final Technical Report

HARDWARE IMPLEMENTATION OF TIME LENSES AND ULTRAFAST OPTICAL TEMPORAL PROCESSORS

Phase I: Feasibility Study

Contract No.: F49620-93-C-0062

Sponsor Agency:

Ballistic Missile Defense Organization

Contract Monitor:

Dr. Alan Craig
Air Force Office of Scientific Research
AFOSR/NE
110 Duncan Avenue, Suite B115
Bolling AFB, DC 20332-0001
(202)-767-4931

Contractor:

Quantex Corporation
2 Research court
Rockville, Maryland 20850
(301)-258-2701

Principle Investigator: Xiangyang Yang

Reporting Period: September 1, 1993 - February 28, 1994

TABLE OF CONTENTS

LIST OF FIGURES AND TABLES

1. INTRODUCTION

The objective of the reported work has been to develop optical hardware implementation of novel time lenses and temporal processors for ultrafast data processing. It was funded by the Ballistic Missile Defense Organization and managed by the Air Force Office of Scientific Research under contract F49620-93-C-0062. The performance period of the Phase I effort was from September 1, 1993 to February 28, 1994.

1.1 Background

Over the last three decades, there have been considerable efforts expended in optical computing and optical signal processing. Various optical computing architectures have been proposed, which are mostly parallel systems with a large number of processing elements to take advantage of the inherent parallelism of optics [1,2]. However, like the limitations imposed by the von Neumann bottleneck on serial processing, there are also fundamental limitations on the possible ultimate speed of parallel processors [3,4]. These limitations include synchronization problems caused by unequal pathways of optical signals [3] and temporal blurring of the light pulse [4]. When a parallel optical computer system approaches its parallel speed limitation, the only way to further boost its performance is to increase the serial processing speed of each processing element. Therefore, ultrafast serial optical processors need to be developed. These high speed processors can also be used to compress the blurred optical pulses and, consequently, to promote the parallel performance of optical computing systems.

In recent years, optical fiber communication technology has been highly successful in implementation and commercialization in telecommunications. This success has spurred the development of optical interconnect technology to solve the problem of high rate, high throughput data transfer between computation modules in modern supercomputers. One of the motivations of optical communication and optical interconnects stems from the high bandwidth of optics [5]. Nevertheless, the huge bandwidth of optics cannot be fully utilized unless the ultrashort pulse generation, compression, and amplification can be performed optically. Recently, much attention has been paid to optical amplifiers which eliminate the need of optic-to-electronic and electronic-to-optic conversions in repeaters in communication networks [6]. But optical processors for distortionless compression and expansion of optical waveforms are yet to be developed.

The optical temporal processors based on time lenses provide a solution to these problems. The innovation of the time lens is based on the analogy between optical spatial diffraction and temporal dispersion [7]. The slowly varying envelope equations corresponding to modulated plane waves in dispersive media have the same form as the paraxial equations describing the propagation of monochromatic waves of finite spatial extent (diffraction). There is a correspondence between the time variable in the dispersion problem and the transverse space variable in the diffraction problem. The essence of the analogy can be stated in short: the temporal frequency corresponds to the spatial frequency in the lateral direction and the time t corresponds to the z coordinate along the optical axis.

This space-time duality has been used in optical pulse compressors [8-10]. In these pulse compressors, a frequency chirp (quadratic time-varying phase shift across the temporal envelope of the pulse) is imparted to a wide input pulse. The quadratic chirp is entirely equivalent to the action of a thin spatial lens [11]. The chirped pulse then passes through a dispersive delay line, which is analogous to free-space propagation in the spatial case. After a suitable time delay (corresponding to the focal length of the spatial lens), the Fourier transform of the input pulse envelope can be detected, which is generally narrower than the original pulse. Therefore, pulse compression is achieved.

Recently this temporal pulse compressor was improved by adding another dispersive delay line before the chirp modulator [12]. This modified configuration is called a *time lens*. An advantage of the time lens over conventional pulse compressors is that it can produce not only the Fourier transform of the input profile, but also a compressed (or expanded) replica of the input pulse. The concepts of time lens and temporal imaging extend our knowledge of optics from the space-domain into the time-domain. Novel temporal imaging and signal processing systems can be created that mimic the operation of their spatial counterparts in the space-domain. A distinct advantage of such temporal processing systems is their extremely high speed (up to picosecond range with currently available devices), which makes it possible to fully utilize the huge bandwidth offered by optics. These processors are able to restore the blurred optical pulses in optical computers, to perform ultrahigh speed serial signal processing, and to compress and expand optical waveforms nearly distortionless. Such temporal processors, if successfully developed, will have a significant impact on optical computing, optical signal processing, and optical communication technologies.

1.2 Phase I research Objectives

The goal of the proposed effort has been to develop optical hardware implementation of novel time lenses and temporal processors. The objective of the Phase I work was to determine the technical feasibility and to perform the architectural design employing off-the-shelf devices. In order to achieve this goal, the following objectives were pursued:

1. Study of space-time duality and temporal imaging concept.
2. Design of time lenses with off-the-shelf devices.
3. Architectural design of temporal imaging and processing systems employing the designed time lenses.
4. Investigation of Applications of the time lenses and temporal imaging and processing systems.
5. Preliminary design of a deliverable prototype temporal microscope.

2. RESEARCH PERFORMED AND RESULTS OBTAINED

During the Phase I period, we studied the space-time duality and established the theoretical model for temporal imaging. Time lenses and several temporal imaging and processing

systems have been designed based on off-the-shelf optical and optoelectronic devices. The properties and performance potentials of these systems have been studied. A temporal microscope is identified for Phase II prototype development. The effort performed and the results obtained are reported in the following sections.

2.1 Space-Time Duality and Temporal Imaging

2.1.1 Spatial diffraction under paraxial approximation

The modern diffraction theory is based on electromagnetic theory and Maxwell's equations [13]. If we denote the amplitude of an optical field by $\psi(x,y,z)$, it obeys the wave equation when propagating in free space:

$$\nabla^2\psi + k\psi^2 = 0 \qquad (1)$$

For simplicity, we assume the amplitude is uniform along y-direction and therefore the optical field is described by $\psi(x,z)$. A general plane-wave solution of the wave equation is of the form:

$$\psi(x,z) = e^{-jk_x x}e^{-jk_z z} \qquad (2)$$

with

$$k_x^2 + k_y^2 = k^2 = \frac{(2\pi f)^2}{c^2} = (\frac{2\pi}{\lambda})^2 \qquad (3)$$

If the propagation vector $\boldsymbol{k}$ is inclined by a small angle with respect to the z-axis, then the wave vector is *paraxial*, and

$$k_z = \sqrt{k^2 - k_x^2} \approx k - \frac{k_x^2}{2k} \qquad (4)$$

This is the paraxial approximation. Henceforth we shall limit our discussion to the cases that satisfy this restriction. We shall further define

$$\psi(x,z) = u(x,z)e^{-jkz} \qquad (5)$$

and use $u(x,y,z)$ as the amplitude distribution. When equation (5) is introduced into the wave equation (1), one obtains:

$$\frac{\partial^2 u}{\partial x^2} + \frac{\partial^2 u}{\partial z^2} - 2jk\frac{\partial u}{\partial z} = 0 \qquad (6)$$

Because $\left|(\partial/\partial z)u\right| << ku$, the term $\partial^2 u/\partial z^2$ is negligible and the *paraxial wave equation* is expressed as:

$$\frac{\partial^2 u}{\partial x^2} - 2jk\frac{\partial u}{\partial z} = 0 \qquad (7)$$

Solving this paraxial wave equation, the amplitude distribution is obtained:

$$u(x,z) = e^{jkz} \int_{-\infty}^{\infty} U|_{z=0}(f_x,z) e^{-j\pi\lambda f_x^2 z} e^{-j2\pi x f_x} df_x \qquad (8)$$

where f_x is the spatial frequency defined as [11]:

$$f_x = \frac{x}{\lambda z} \qquad (9)$$

The function $U|_{z=0}(f_x,z)$ is the Fourier transform of the amplitude distribution at $z=0$:

$$U|_{z=0}(f_x,z) = U(f_x,0) = \int_{-\infty}^{\infty} u(x,0) e^{j2\pi x f_x} dx \qquad (10)$$

Equations (8) and (10) describe the propagation properties of an optical field and are the foundation of the Fourier optics [11]. It is seen from equation (8) that the diffracted optical field can be expressed by the Fourier transform of the aperture function.

From the view point of Fourier optics, an optical lens is merely a phase modulator described by:

$$l(x) = e^{-j\frac{kx^2}{2F}} = e^{-j\frac{\pi x^2}{\lambda F}} \qquad (11)$$

where F is the focal length of the lens. It modulates the phase of the input wave front in such a way that an image of the input object is formed at a certain distance behind it, and the Fourier transform of the input optical field is obtained at its back focal plane [11].

2.1.2 Temporal dispersion of narrow band optical waves

The discussion in the preceding section is only for monochromatic optical waves, or polychromatic optical waves propagating in a non-dispersive media. Now, let us consider the propagation of a polychromatic plane wave in a dispersive media. Assume the temporal spectrum occupies only a narrow band around frequency f_o. The spectrum of the plane wave propagating in z-direction is expressed as

$$U(f,z) = U(f) e^{-jk(f)z} \qquad (12)$$

where

$$k = 2\pi f \sqrt{\mu\varepsilon} \qquad (13)$$

The time-dependent optical field is obtained by taking a Fourier transform:

$$u(t,z) = \int_{-\infty}^{\infty} U(f) e^{j[2\pi ft - k(f)z]} df \qquad (14)$$

In a dispersive media, ε is a function of f and thus k is not simply proportional to f. We may expend k in the neighborhood of f_o to first order in $\Delta f = (f - f_o)$ and ignore higher-order terms, because they contribute negligibly to the integral owing to the narrow band assumption. Thus,

$$k(f) \approx k(f_o) + \left.\frac{dk}{df}\right|_{f_o} \Delta f \qquad (15)$$

Substitute (15) into (14), we have:

$$u(t,z) = e^{j[2\pi f_o t - k(f_o)z]} \int_{band} U(\Delta f) e^{j\Delta f[2\pi t - (dk/df)z]} d\Delta f \qquad (16)$$

Equation (16) shows that the z-dependence of u(t,z) consists of two factors:

1. A rapidly varying term, the carrier, that propagates with the *phase velocity* $f_o / k(f_o)$.
2. A slowly varying envelop that proceeds with the *group velocity* $df/dk = 1/(dk/df)$.

For a nondispersive medium, the two velocities are the same, but not for a medium with an ε that depends on frequency, a dispersive medium. When a narrow band optical pulse propagates through a dispersive medium, different frequency components travel at different speed. After traveling a distance, the profile of the pulse is changed due to the dispersion.

It should be noted that the foregoing derivation of the group velocity is not limited to a plane wave, but applies to any linear process with a spatial dependence *exp[-jk(f)z]* at frequency f. This assures the validity of our discussion later in this report, where the modulated optical wave may propagate through optical fibers, or grating pairs.

2.1.3 Space-time duality

we further define the complex envelop of the optical pulse as:

$$a(t,z) = \int_{band} U(\Delta f) e^{j\Delta f[2\pi t - (dk/df)z]} d\Delta f \qquad (17)$$

Then, the propagation of a narrow band optical pulse can be treated as the propagation of a varying envelop with its single nominal frequency f_o.The differential equation that governs the propagation of the envelop is

$$\left(\frac{\partial}{\partial z} + \frac{1}{v_g}\frac{\partial}{\partial t}\right) a(t,z) = \frac{j}{2}\frac{d^2k}{df^2}\frac{\partial^2 a(t,z)}{\partial t^2} \qquad (18)$$

where $$v_g = \frac{1}{\frac{dk}{df}} \qquad (19)$$

is the group velocity, i.e., the velocity at which the pulse envelop propagates. The envelop *a(t, z)* would propagate unchanged at the group velocity were it not for the term on the right-hand side, which produces "distortion". Note that this term is imaginary and, therefore, it contributes to the phase.

There is a qualitative interpretation of the term d^2k/df^2. It is a measure of the velocity change within the bandwidth. One may treat an optical pulse as made up of many spectral components occupying the total bandwidth. Each of the pulse components has its own group velocity which varies over the width of the spectrum. Over a travel distance, some components are left behind while some other components rush ahead. This leads to the change in the profile of the envelop.

The equation for pulse propagation in a dispersive medium can be made to bear an uncanny resemblance to the paraxial wave equation. For that purpose, we introduce a new variable

$$\tau = t - \frac{z}{v_g} \qquad (20)$$

which is a measure of the change in pulse shape corresponding to a moving point at position z. Note that $d\tau = 0$ when $dt = dz/v_g$, i.e., when the position z is changed at the rate v_g. With the new variable τ, we can write equation (18) in the form:

$$\frac{\partial^2 a}{\partial x^2} + 2j\frac{1}{\frac{d^2k}{df^2}}\frac{\partial a}{\partial z} = 0 \qquad (21)$$

It is of the same form as the paraxial wave equation (7). Hence, the solutions must be identical with those the paraxial wave equation and the spatial lens and spatial imaging should have their counterparts in the temporal domain. Comparison of the paraxial wave equation (7) with the narrow band pulse propagation equation (21) leads to the correspondences between the diffraction and dispersion, i.e., the *space-time duality*, as shown in Table 2.1. One must note that d^2k/df^2 can be either positive (normal dispersion) or negative (anomalous dispersion). This can be taken into account by the sign of k assigned to the paraxial wave solution.

Let us consider the propagation of an initial signal *u(t, z=0) in a dispersive medium*. If the initial spectrum is denoted as *U(f, z=0)*, the pulse can be expressed as:

Table 2.1 Space-Time Duality

Paraxial Diffraction	Pulse Dispersion
$u(x, z)$	$a(\tau, z)$
z	z
x	$t = t - z/v_g$
k	$2\pi (d^2k\ df^2)$
λ	$k_2 = d^2k\ df^2$
f_x	Δf

$$u(t,z)\big|_{z=0} = \int_{-\infty}^{\infty} U(f,z)\big|_{z=0} e^{j2\pi ft} df \qquad (22)$$

Again, we assume the temporal spectrum occupies only a narrow band around frequency f_o. Then equation (22) can be written as:

$$u(t,0) = e^{j2\pi f_o t} \int_{band} U(\Delta f,0) e^{j2\pi \Delta f t} d\Delta f \qquad (23)$$

where $\Delta f = f - f_o$. We may expand k in the neighborhood of f_o to the second order in Δf and ignore higher order terms owing to the narrow band assumption:

$$k(f) = k\big|_{f_o} + \left.\frac{dk}{df}\right|_{f_o} \Delta f + \frac{1}{2}\left.\frac{d^2k}{df^2}\right|_{f_o} \Delta f^2 \qquad (24)$$

$$= k_o + k_1 f + \frac{1}{2} k_2 f^2 \qquad (25)$$

where

$$k_o = k(f_o) = 2\pi f_o \sqrt{\mu\varepsilon(f_o)} \qquad (26)$$

$$k_1 = \left.\frac{dk}{df}\right|_{f_o} = \frac{1}{v_g(f_o)} \qquad (27)$$

$$k_2 = \left.\frac{d^2k}{df^2}\right|_{f_o} = \frac{d}{df}\left(\frac{1}{v_g}\right)\Big|_{f_o} \qquad (28)$$

A traveling wave with a monofrequency f will experience a phase delay when propagating along a distance z:

$$e^{j2\pi\Delta\varphi} = e^{j2\pi[ft - k(f)z]}$$

$$= e^{j2\pi f_0 t} \cdot e^{j2\pi M[t-k_1 z]} \cdot e^{j\pi k_2 M^2 z} \qquad (29)$$

The first factor in equation (29) determines the phase velocity and is frequency independent. The second factor describes the group velocity of the optical pulse along z direction. The third factor is related to the change in group velocity for different frequency components, or simply the dispersion. It is this dispersion factor that causes distortion of the signal. The pulse at distance z can be expressed as:

$$u(t,z) = \int_{-\infty}^{\infty} U(f,0) e^{j\Delta\phi(t,z)} df$$

$$= e^{j2\pi f_0 t} \int_{band} U(\Delta f,0) e^{-j\pi k_2 M z} e^{-j2\pi\Delta f t} \qquad (30)$$

Comparing equation (30) with (8), we see that the equations governing the paraxial diffraction and the narrow band dispersion have exact mathematic form. The temporal frequency Δf corresponding the spatial frequency f_x, and the temporal wavelength λ corresponds to the dispersion k_2. Other correspondences between the spatial parameters in diffraction and temporal parameters in dispersion are summarized in Table 2.1.

2.1.4 Time lens and temporal imaging

Based on space-time duality, the concepts of lens and imaging can be extended from the spatial domain to the temporal domain. A lens in the space domain is a phase modulator characterized by equation (11) in Section 2.1.1. Considering the analogous parameters listed in Table 2.1, a *time lens* can be defined in the time domain as:

$$l(\tau) = e^{-j\frac{\pi\tau^2}{k_{2l}F}} \qquad (31)$$

where k_{2l} stands for the dispersion characteristics of the device that implements the time lens, and F denotes the temporal focal length. A time lens could be analogous to a convex or a concave spatial lens, if k_{2l} is positive or negative. It should be noted that the parameter τ is measured from a moving observation point that travels at the nominal group velocity. In order to use the tools and methods developed in Fourier optics, it is useful to express the time lens by its Fourier spectrum:

$$L(\Delta f) = \int_{-\infty}^{\infty} l(\tau) e^{-j2\pi\tau M} d\tau = \sqrt{k_2 F} \cdot e^{-j\frac{\pi}{4}} \cdot e^{j\pi k_2 F M^2} \qquad (32)$$

It is characterized by a quadratic phase term in the spectrum domain. Therefore, a time lens is in fact a chirp modulator.

The space-time image analogy is schematically illustrated in Fig.1. The conventional spatial imaging system consists of three subsystems in cascade: free space propagation, modulation by the lens, and again free space propagation. We arrange the temporal imaging

system in a similar way. A temporal signal (e.g., an optical pulse) travels over a distance z_o in a dispersive medium, interacts with the time lens, and then propagates over a distance z_i in another dispersive medium. The dispersive media shown in Fig.1(b) are also called dispersive delay lines of lengths z_o and z_i, respectively, since they lead the delays between different spectral components after the optical pulse travels through them.

In general, the dispersive media before and behind the time lens have different dispersion properties, which can be characterized by k_{2o} and k_{2i}, respectively. The subscript o stands for the object side; whereas the subscript i stands for the image side. The signal traveled through the first dispersive delay line at just before the time lens is:

$$u(\tau, z_{o-}) = e^{j\frac{2\pi f_o z_o}{v_g}} \int U(\Delta f, 0) e^{-j\pi k_{2o} \Delta f^2 z_o} e^{j2\pi \Delta f \tau} d\Delta f \qquad (33)$$

From now on, the limitation for integrations are always from minus infinity to infinity if not specifically mentioned. The action of the time lens is to modulate the phase of the input signal. For the sake of simplification, we prefer to express a time lens in the form of Fourier integral. Thus, the signal at the position immediately behind the lens can be written as:

$$u(\tau, z_{i-}) = \sqrt{k_{2i} F} e^{-j(\frac{2\pi f_o z_o}{v_g} + \frac{\pi}{4})} \iint U(\Delta f, 0) e^{-j\pi k_{2o} \Delta f^2 z_o} e^{j2\pi \Delta f \tau} e^{j\pi k_{2i} F \rho^2} d\rho \, d\Delta f \qquad (34)$$

After propagating a distance z_i, the output signal is:

$$u(\tau, z_o + z_i) = \sqrt{k_{2i} F} e^{-j(\frac{2\pi f_o (z_o + z_i)}{v_g} + \frac{\pi}{4})} \iint U(\Delta f, 0) e^{-j\pi k_{2o} \Delta f^2 z_o} e^{j2\pi \Delta f \tau} e^{j\pi k_{2i} F \rho^2} e^{-j\pi k_{2i} (\Delta f + \rho)^2 z_i} e^{j2\pi \rho \tau} d\rho d\Delta f$$

$$= \sqrt{\frac{k_{2i} F}{k_{2i} z_i - k_{2i} F}} e^{-j\frac{2\pi f_o (z_o + z_i)}{v_g} - \frac{\pi}{2})} \int U(\Delta f, 0) e^{-j\pi (k_{2o} z_o + k_{2i} z_i) \Delta f^2} e^{j\frac{\pi (k_{2i} z_i \Delta f - \tau)^2}{k_{2i} z_i - k_{2i} F}} e^{j2\pi \Delta f \tau} d\Delta f \qquad (35)$$

The definition of Dirac function was used in the derivation of equation (35). In order to obtain an image at position z_i, the Δf^2 term in the integral should be zero. That is:

$$-j\pi(k_{2o} z_o + k_{2i} z_i) + j\frac{\pi (k_{2i}^2 z_i^2}{k_{2i} z_i - k_{2i} F} = 0 \qquad (36)$$

This leads to the imaging equation:

$$\frac{1}{k_{2o} z_o} + \frac{1}{k_{2i} z_i} = \frac{1}{k_{2i} F} \qquad (37)$$

Compare (37) with spatial imaging equation:

$$\frac{1}{z_o} + \frac{1}{z_i} = \frac{1}{F} \qquad (38)$$

The analogy between temporal imaging and spatial imaging is amazingly obvious. Substitute (36) into (35), we have:

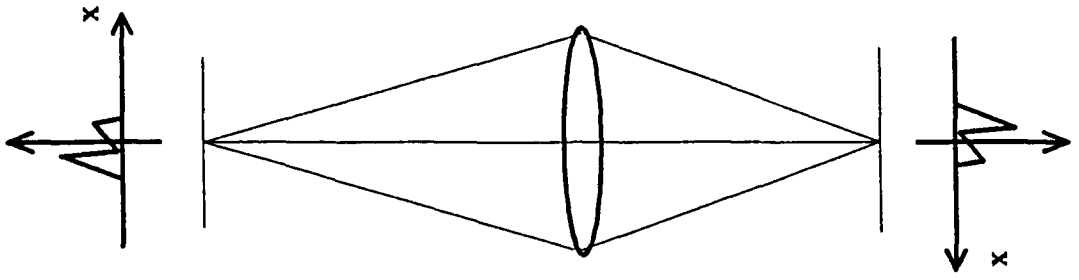

(a)

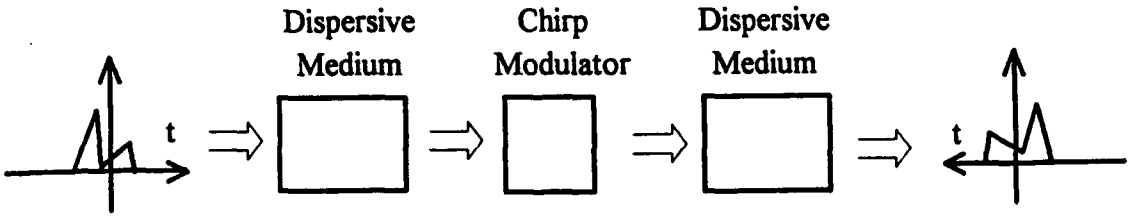

(b)

Fig. 1 Space-time imaging analogy, (a) spatial imaging configuration, (b) temporal imaging configuration.

$$u(\tau, z_o + z_i) = \sqrt{\frac{k_{2o} z_o}{k_{2i} z_i}} e^{-j(\frac{2\pi f_o (z_o + z_i)}{v_g} + \frac{\pi}{2})} e^{j\frac{\pi \tau^2}{k_{2i} z_i - k_{2i} F}} \int U(\Delta f, 0) e^{-j2\pi \frac{k_{2o} z_o}{k_{2i} z_i} \Delta f \tau} d\Delta f$$

$$= \sqrt{\frac{k_{2o} z_o}{k_{2i} z_i}} \cdot e^{-j(\frac{2\pi f_o (z_o + z_i)}{v_g} + \frac{\pi}{2})} \cdot e^{j\frac{\pi \tau^2}{k_{2i} z_i - k_{2i} F}} \cdot u(-\frac{k_{2o} z_o}{k_{2i} z_i}) \qquad (39)$$

This is the image of the input signal except for a phase chirp described by the third term, which corresponds to the phase curvature in spatial imaging [11]. If the output pulse is detected by a photodetector, the detected intensity is:

$$I(t, z_o + z_i) = \frac{k_{2o} z_o}{k_{2i} z_i} \left| u(-\frac{k_{2o} z_o}{k_{2i} z_i} \tau, 0) \right|^2 = \frac{k_{2o} z_o}{k_{2i} z_i} I(-\frac{k_{2o} z_o}{k_{2i} z_i} \tau, 0) \qquad (40)$$

The term $k_{2o} z_o \, k_{2i} z_i$ verifies the law of energy conservation. The magnification, i.e., the change in pulse width, is

$$M = \frac{k_{2i} z_i}{k_{2o} z_o} \qquad (41)$$

Although the chirp term does not have any contribution to the intensity, it does modulate the phase of the output signal. This phase modulation must be taken into account in the design of complex temporal imaging systems where a number of time lenses are cascaded.

Similar to spatial imaging, the Fourier transform spectrum can be obtained at the back focal plane of a time lens. It should be noted that the focal length, as well as the object and image distances, is determined by both the dispersive and dimensional parameters. Therefore, that the image distance equals to the focal length means the following relationship:

$$k_{2i} z_i = k_{2i} F \qquad (42)$$

Substitute (42) into (35), we have:

$$u(\tau, z_o + F) = \sqrt{k_{2i} F} e^{-j\frac{2\pi f_o (z_o + z_i)}{v_g} - \frac{\pi}{4})} \iint U(\Delta f, 0) e^{-j\pi (k_{2o} z_o + k_{2i} F) \Delta f^2} e^{j2\pi \Delta f \tau} e^{-j2\pi k_{2i} F \Delta f \rho} e^{j2\pi \rho \tau} d\rho d\Delta f \qquad (43)$$

$$= \sqrt{k_{2i} F} \cdot e^{-j(\frac{2\pi f_o (z_o + z_i)}{v_g} + \frac{\pi}{4})} \cdot e^{j\pi \frac{(k_{2o} z_o - k_{2i} z_i) \tau^2}{k_{2i}^2 F^2}} \cdot U(\frac{\tau}{k_{2i} F}, 0) \qquad (44)$$

It is seen that the output at the back focal plane is a scaled version of the temporal Fourier transform of the input signal, as is expected from the dual spatial case. The chirp term, which corresponds to the phase curvature in spatial spectral analysis, disappears only when the input is at the front focal plane, i.e.,

$$k_{2,out} z_{out} = k_{2,in} l \qquad (45)$$

This is the analogy of the so called 2-f system in Fourier optics. A 4-F system can be formed by cascading two 2-F systems. If such two 2-f system have different focal lengths, an enlarged or reduced image can be obtained at the output plane without the phase chirp. Temporal filtering can be carried out by manipulations at the back focal plane of the first 2-f system. Such applications of the time lens will be discussed later in this report.

2.2 Design of Time Lenses with Off-the-Shelf Devices

It is shown in Fig.1(b) that a basic temporal imaging system consists of a time lens and two dispersive delay lines. During the Phase I effort, we have designed time lenses with electro-optic phase modulators, and dispersive delay lines with diffraction grating pairs. The working wavelength was chosen to be 670 nm. The design criteria are discussed in this section.

2.1.1 Design of time lenses

A time lens is essentially a chirp phase modulator and can be implemented by several devices, such as optical fibers [8] and electro-optic modulators [9,10]. To ensure a large dynamic range, a constant degree of quadratic phase modulation, independent of input pulse parameters, is desired. Nevertheless, the self phase modulation (SPM) in an optical fiber is power dependent [15]; thus the electro-optic modulator is more favorable. Moreover, electro-optic modulators offer an additional advantage in that the sign of the chirp is controllable, and therefore, optical elements with either positive or negative group-velocity dispersion can be used in the system. Electro-optic modulators with bandwidth up to 18 GHz are currently available from New Focus [16], United Technologies Photonic Inc., and other manufacturers.

Assume the electro-optic phase modulator is driven by a sinusoidal voltage of frequency f_m. If the input optical waveform is shorter than $1/f_m$, then the phase modulation is essentially quadratic under any extremum of the sinusoid [10]. On leaving the modulator, the pulse has acquired a phase shift:

$$\phi(t) = A(1 - 2\pi^2 f_m^2 t^2) \qquad (45)$$

where A is the modulation index or peak phase deviation and can be either positive or negative depending upon whether the pulse is positioned under the region of positive or negative curvature. Note that since the phase is quadratic in time, the instantaneous frequency has a linear chirp given by:

$$\frac{\partial^2 \phi}{\partial t^2} = -4\pi^2 A f_m^2 \qquad (46)$$

To design a time lens with such a electro-optic phase modulator, let:

$$l(\tau) = e^{j\frac{\pi \tau^2}{k_2 F}} = e^{-j2\pi^2 A f_m^2 \tau^2} \qquad (47)$$

We have:

$$k_{2l}F = \frac{1}{2\pi A f_m^2} \qquad (48)$$

The characteristics, more specifically, the focal length of the time length is determined by the modulation index and working frequency of the electro-optic modulator. The dependency of the focal length on the modulation index and drive frequency is illustrated in Fig.2.

An electro-optic phase modulator available from New Focus Inc (model No. 4861) has been chosen for the implementation of time lens. Its operation frequency is upto 10 GHz and the peak modulation index at 670 nm is 32 rad [16]. Substitute these parameters into (48) focal length of such a time lens is:

$$k_{2l}F = \frac{10^{2}}{64\pi} \approx 4.97 \times 10^{-3} \qquad (\sec^2) \qquad (49)$$

The modulators having larger modulation index and higher operational frequency is expected to be available in the next year (1995), which will lead to time lenses with shorter focal lengths.

2.1.2 Design of dispersive delay lines

The dispersive delay line can be implemented with a diffraction grating pair [17] or by using the self phase modulation (SPM) effect in an optical fiber [15]. When an optical fiber is used, it should have a large group velocity dispersion value in order to generate the dispersion efficiently [18]. However, all the fibers for communication purposes are optimized for low dispersion value. In other words, we need what are called *bad fibers*. Such fibers are not easy to obtain. The data about these fibers do not appear in the literature either. In contrast, the grating pair approach is relatively mature. The high quality diffraction gratings are available from many providers, such as Newport, Oriel, Spectrogon, etc. Therefore, grating pairs were selected for the implementation of dispersive delay lines.

The phase delay of a plane wave traveling through a pair of parallel, identical gratings is illustrated in Fig.3 We select P as the starting point and Q as the emerging point. Without loss of generality, we assume that the peaks of each of the fundamental Fourier components of the grating corrugations occur at the intersections of the indicated normal. The length AB is defined as:

$$h = \frac{g}{\cos\theta_R} \qquad (50)$$

where g is the spacing of the grating pair. The travel distance is determined by:

$$\overline{PABQ} \equiv p = \frac{g}{\cos\theta_R}[1+\cos(\theta_i + \theta_R)] \qquad (51)$$

Note that θ_R is negative in Fig.3, assuming that the grating reflection is of negative order, $m=-1$.

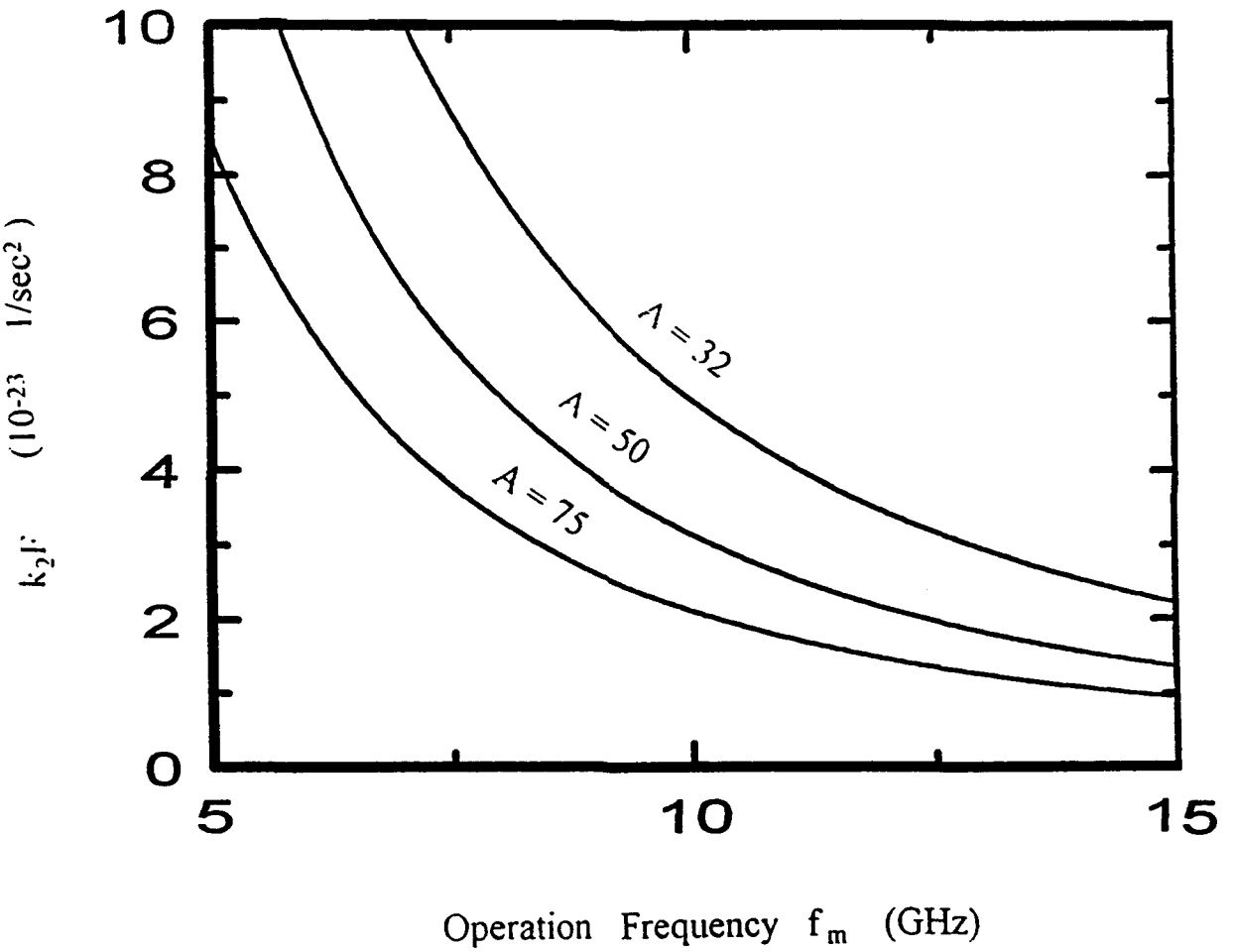

Fig.2 Focal length of the time lens as a function of modulation index, A, and drive frequency, f_m. $k_2F = 1/(2\pi A f_m^2)$.

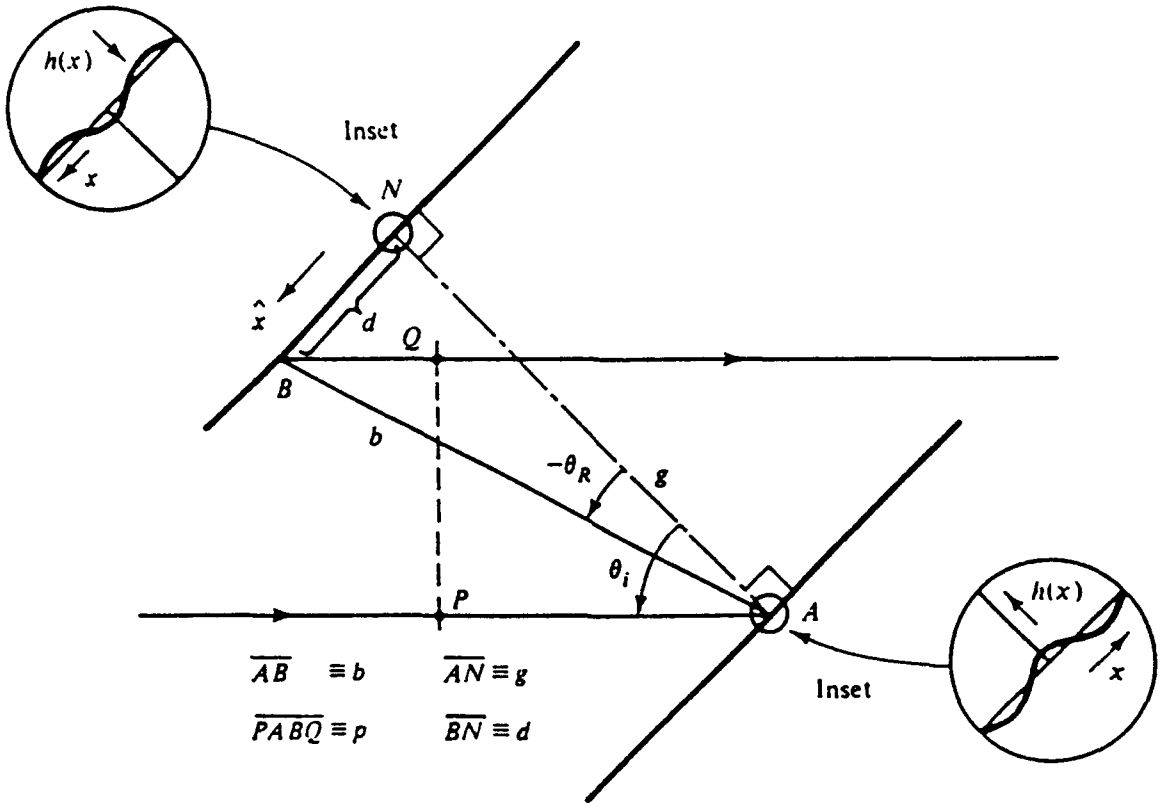

Fig.3 Grating pair as dispersive delay line

The reflection angle θ_R is expressed as:

$$\sin\theta_R = \sin\theta_i - \frac{\lambda}{\Lambda} \qquad (52)$$

where Λ is the period of the grating.

The phase shift of the optical wave over the path PABQ is:

$$\phi(f) = \frac{2\pi f}{c} p \qquad (53)$$

The dispersion produced by the grating is characterized by:

$$\frac{d^2\phi(f)}{df^2} = -\frac{4\pi^2\lambda^3 g}{c^2\Lambda^2}[1-(\sin\theta_i - \frac{\lambda^2}{\Lambda^2})]^{-\frac{3}{2}} \qquad (54)$$

The grating pair acts like a medium with dispersion parameter k_2 and thickness z, with

$$k_2 z = -\frac{1}{2\pi}\frac{d^2\phi(f)}{df^2} = -\frac{2\pi\lambda^3 g}{c^2\Lambda^2}[1-(\sin\theta_i - \frac{\lambda^2}{\Lambda^2})]^{-\frac{3}{2}} \qquad (55)$$

The dominant parameters that determine the dispersion behavior of a grating pair are period of the grating, Δ, and the spacing between the gratings, g. The incident angle, θ_i, has very little influence. As an example, figure 4 shows the normalized object distance, $(k_2 z/g)$, as the function of the period of grating under the incident angle of 60°.

The configuration of a single-lens temporal imaging system based on above design is schematically illustrated in Fig.5. It consists two grating pairs and an electro-optic phase modulator. The spaces of the two grating pairs are suitably arranged such that either the temporal imaging equation (37) is hold for obtaining an image of the input, or equations (42) and (45) are satisfied for obtaining the temporal Fourier transform of the input signal. More complex optical systems can be constructed based on such single-lens systems.

2.3 Architectural Design of Temporal Imaging and Processing Systems

Based on the single-lens configuration shown in Fig.5, we have designed a temporal magnifier, a telecentric temporal microscope, and a 4-f temporal filtering system. The design of these systems are discussed in this section.

2.3.1 Temporal magnifier

A temporal magnifier is basically a single lens system having a configuration the same as that shown in Fig.5. The designed magnifier has a magnification of 100X. An electro-optic phase modulator available from New Focus Inc (model No. 4861) is chosen as the chirp modulator. Its operation frequency is up to 10 GHz, and the peak modulation index at 670 nm is 32 rad [16].

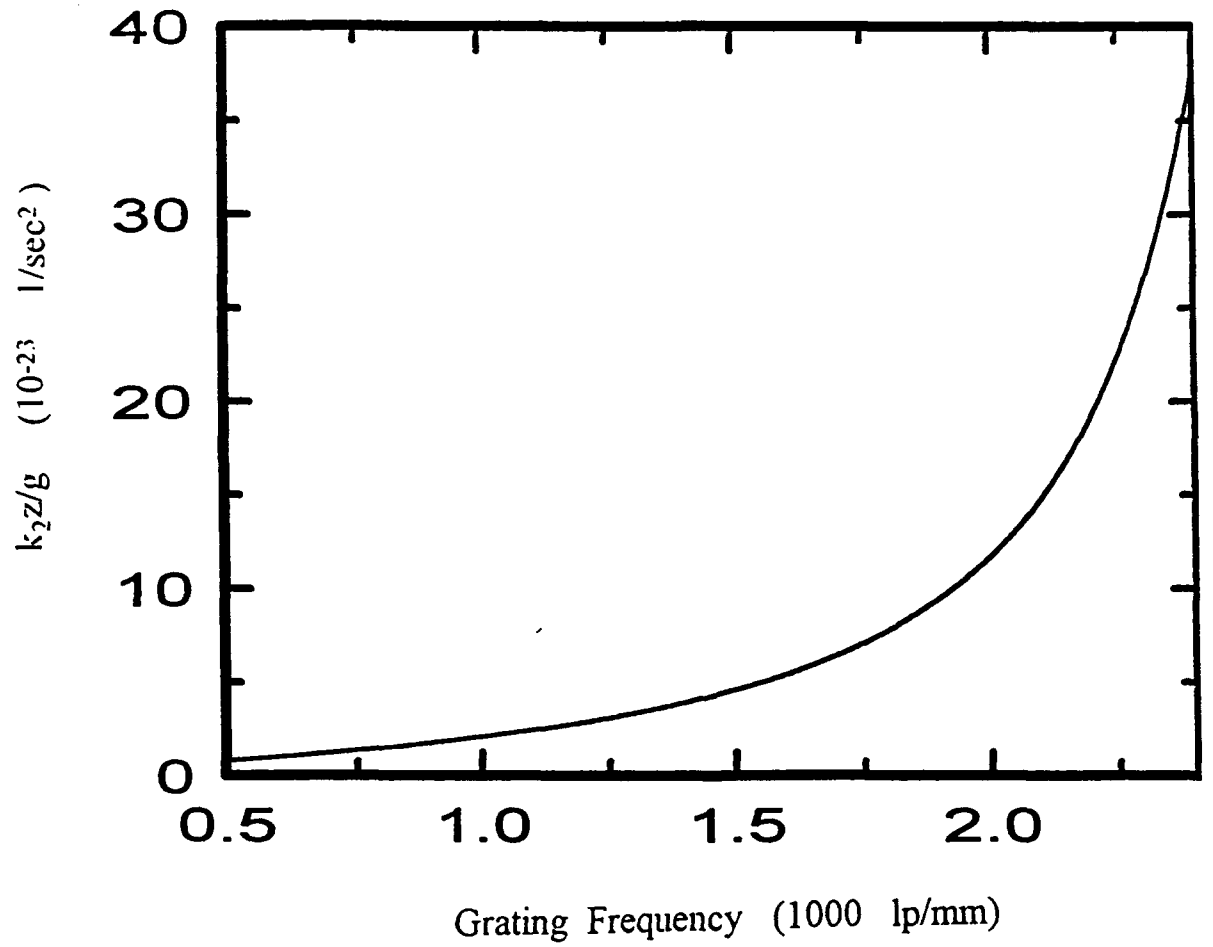

Fig. 4 The normalized object (or image) distance, (k_2z/g), as a function of the period of the grating. Incident angle is 60°.

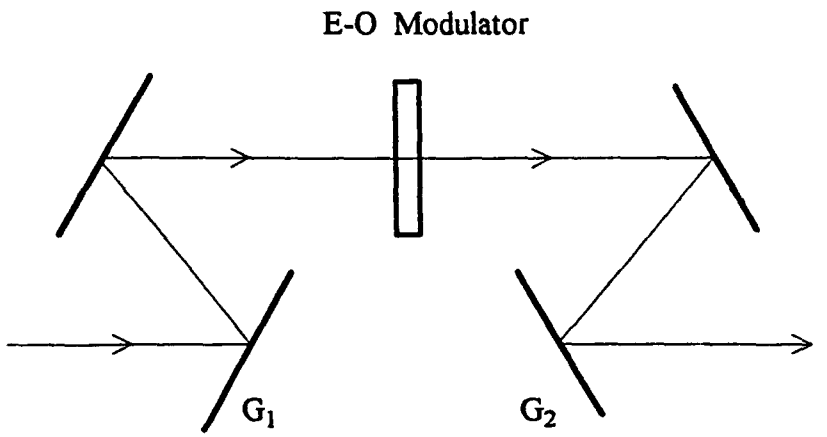

Fig.5 Configuration of a single-lens system consisting of two pairs of gratings and an electro-optic phase modulator.

Substitute these parameters into (48), and the focal length of such a time lens is:

$$k_{21}F = \frac{10^{-20}}{64\pi} \approx 4.97 \times 10^{-23} \qquad (\sec^2)$$

Solving the temporal imaging equation (37) and magnification equation (41), we have:

$$k_{20}z_o = 1.01k_{21}F \approx 5.0233 \times 10^{-23} \qquad (\sec^2)$$

$$k_{21}z_i = 101k_{21}F \approx 5.0233 \times 10^{-21} \qquad (\sec^2)$$

Assume the periods of the grating pairs at the object side and image side are:

$$\Lambda_o = \frac{1}{1500} \qquad (\text{lp/mm})$$

$$\Lambda_i = \frac{1}{2700} \qquad (\text{lp/mm})$$

and the incident angle to the grating pairs is 60° at both sides, the spacings between the grating pairs are obtained from (55):

$$g_o = 1032.4 \qquad (\text{mm})$$

$$g_i = 1198.2 \qquad (\text{mm})$$

Such a magnifier can certainly be used as a demagnifier by alternating the positions of the two grating pairs, i.e., moving the image grating pair into the object side and place the object grating pair in the image side. The magnification will then be 0.01X.

2.3.2 Telecentric temporal microscope

One of the disadvantages of the single-lens system is that a phase chirp is always contained in the output. Although the phase chirp does not have any contribution to the output intensity, it does affect the function of other temporal imaging or processing systems that cascaded with the single-lens magnifier. As discussed in the previous sections, this chirp term disappears when the input and output planes coincide with the front and back focal planes. Therefore, a chirp-free temporal microscope can be constructed by cascading two time lenses into a telecentric system.

Assume the required magnification is 100X. The two time lenses are implemented with two electro-optic modulators working at drive voltage of $f_{m1}=10\ GHz$ and $f_{m2}=1\ GHz$, respectively. Then, the focal lengths of the two time lenses are:

$$k_{21}F_1 = \frac{1}{2\pi A f_{m1}^2} \approx 4.97 \times 10^{-23} \qquad (\sec^2)$$

$$k_{21}F_2 = \frac{1}{2\pi A f_{m2}^2} \approx 4.97 \times 10^{-21} \qquad (\sec^2)$$

The object and image distances are equal to the focal length of the time lens. That is:

$$k_{20}z_{01} = k_{21}z_{11} = k_{21}F_1 \approx 4.97 \times 10^{-23} \quad (\sec^2)$$

$$k_{20}z_{02} = k_{22}z_{12} = k_{22}F_2 \approx 4.97 \times 10^{-21} \quad (\sec^2)$$

To reduce the system complxicity, we combine the grating pairs behind the first lens and before the second lens into a single grating pair. The simplified configuration is shown in Fig.6. Assume the periods of the grating pairs are:

$$\Lambda_1 = \frac{1}{1500} \quad (\text{lp/mm})$$

$$\Lambda_2 = \Lambda_3 = \frac{1}{2700} \quad (\text{lp/mm})$$

If the incident angles to all the grating pairs are 60°, the spacings between the grating pairs are obtained from (55):

$$g_1 = 1022.3 \quad (\text{mm})$$

$$g_2 = 1210.2 \quad (\text{mm})$$

$$g_3 = 1198.2 \quad (\text{mm})$$

2.3.3 4-f temporal filtering system

The most interesting spatial optical processor is the 4-f system for optical filtering and correlation computation [11]. The configuration of a temporal 4-f system is illustrated in Fig.7. It is essentially a telecentric system. The two time lenses have generally the same focal length. The difference from the telecentric microscope is that the two grating pairs between the two time lenses cannot be combined into a single pair, but must be separated. The space between these two grating pairs is the so called spectrum domain and is reserved for all the filtering operations [18].

The two time lenses have identical configurations in the designed temporal 4-f system. Again, the New Focus' electro-optical modulators (model No. 4841) are used as chirp modulator. Assume the drive frequency is 10 GHz and the peak modulation index is 32 rad., the focal length of such a time lens is:

$$k_{21}F = \frac{1}{2\pi A f_m^2} \approx 4.97 \times 10^{-23} \quad (\sec^2)$$

To eliminate the phase chirp at the focal plane, let:

$$k_{20}z_0 = k_{21}z_1 = k_{21}F \approx 4.97 \times 10^{-23} \quad (\sec^2)$$

The period of all the grating pairs is:

$$\Lambda = \frac{1}{1800} \quad (\text{lp/mm})$$

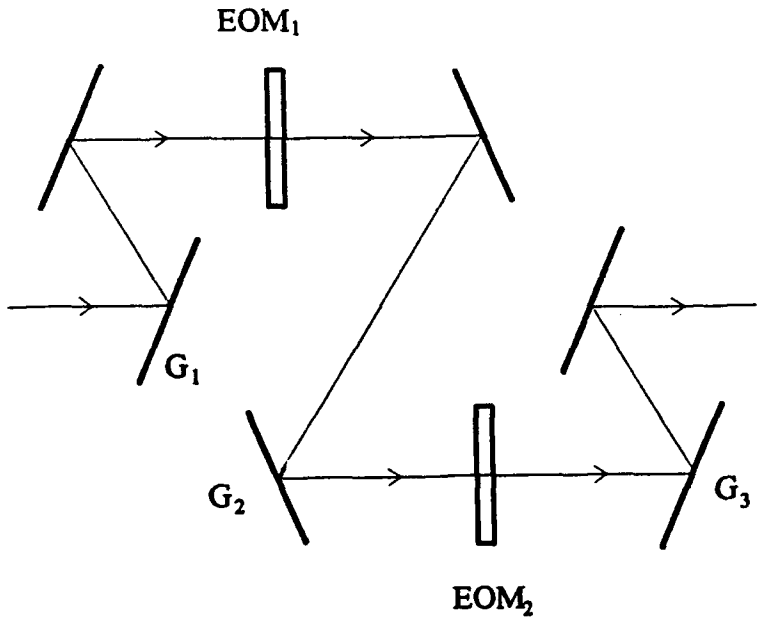

Fig.6 Configuration of a telecentric temporal microscope

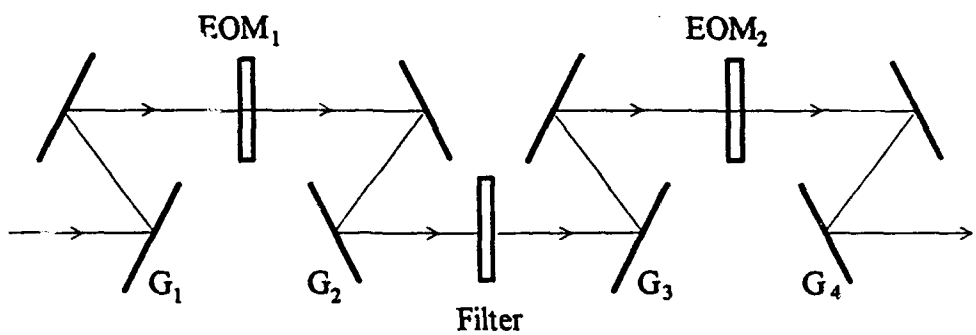

Fig. 7 Configuration of a temporal 4-f filtering system

The incident angle to the grating pairs is 60° at both sides of the time lens. Then, the spacing between each grating pair is:

$$g = 608 \quad (\text{mm}).$$

The spectral bandwidth of this 4-f system is determined by the parameters of the electro-optic modulator:

$$W_f = \frac{1}{2k_1 l} = \pi A f_m^2 \qquad (56)$$

When fm=10 GHz, A=32, the spectral bandwidth is:

$$W_f = 1.005 \times 10^{12} \quad (\text{Hz})$$

The terahertz bandwidth meets the requirements of optical communication systems. According to the Sampling theorem, the time resolution is inversely proportional to the spectral bandwidth. That is:

$$\Delta\tau = \frac{1}{W_f} = 0.995 \times 10^{-12} \quad (\text{sec})$$

Subpicosecond resolution can be achieved in such a temporal processing system. The input aperture is limited by the space between the grating pairs:

$$W_\tau = \frac{g}{v_g} = 0.203 \times 10^{-9} \quad (\text{sec})$$

The time-bandwidth-product (TBP) of the system is:

$$TBP = W_\tau \cdot W_f = 2040$$

Such a TBP can meet the needs of most temporal filtering applications.

2.4 Application Investigation

The applications of time lenses abound. The temporal imaging system immediately suggests new geometries that can enhance the versatility and improve the performance of pulse compressors. Any particular optical waveforms could be prepared on a long time scale and then compressed for applications in coherent spectroscopy [19] and nonlinear pulse propagation experiments, such as soliton communication experiments [15]. Optimum long pulse shapes could also be prepared for high-power amplification and subsequent compression. If the magnification of the imaging system is much greater than one, temporally expanded distortionless replicas of high-speed optical waveforms can be produced with a temporal microscope. It could extend the range of direct optical measurements with ordinary high-speed photodetectors and oscilloscopes to a regime that is so far accessible only with streak cameras or nonlinear optical techniques. For communication applications, data streams could be encoded at nominal rates and compressed and multiplexed for high-density optical communications. Since the high-rate data stream is generated fully optically, the full utilization of the huge bandwidth offered by optics can be expected. The

temporal correlators provide an effective means to deal with ultrafast temporal signals, or even transient signals. They are especially useful for applications in radar and sonar signal processing, DNA sequence analysis, space and satellite communications, etc. Two possible applications of time lenses are discussed in this section.

2.4.1 Temporal microscope for picosecond optical pulse profile measurement

The rapid progress of short-pulse laser technology has produced a concomitant increase in the use of ultrashort laser pulses for measuring various transient phenomena. The advantage of using ultrashort laser pulses is the high temporal resolution they offer. As the time duration of the phenomena under investigation approaches the optical pulse widths that are used to measure them, accurate information on the optical pulse profile becomes critically important.

Streak cameras has been used to measure laser pulse shape for many years. Since the fastest response time of the streak camera is larger than 1 ps, it cannot be used to characterize picosecond laser pulses [20]. All the other techniques employ nonlinear optical interaction and their practical applications are rather limited. The commonly used intensity autocorrelation does not preserve the phase information of the pulse, so that any asymmetries will not be recovered from the measured signal [21]. Interferometric auto-correlation techniques require additional measurements (and equipment) to completely describe an optical pulse, thereby increasing the cost and complexity of analysis [22]. Other double correlation techniques require nonlinear processes to modify the pulse in one (or both) of the arms of an autocorrelator [23]. Unless these processes are well characterized, it will be impossible to accurately reconstruct the input pulse.

The degenerate four-wave mixing method uses the correlation of three replicas of the input pulse to keep the phase information [24]. The drawback of this technique is its use of the third-order nonlinear susceptibilities, which are often so small as to require pump intensities that approach, or even exceed, the damage threshold of the nonlinear materials [25]. A new triple correlation technique was recently proposed that uses two consecutive second-order nonlinear optical interactions to determine the pulse profile [26,27]. In order to acquire the 2-D correlated data, a series of measurements corresponding to different time delays among the three pulse replicas must be made. The data acquisition is time consuming and mechanical movement is required to generate various time delays. Moreover, if the shapes of pulses in the pulse series are not identical, or if the pulse shape changes during the data acquisition process, the output is erroneous.

To overcome these difficulties, the temporal microscope discussed in the preceding Section can be used as en effective tool for the profile measurement of ultrashort optical pulses. The temporal microscope generates a temporal image of the input pulse. The image preserves exactly the shape, or profile, of the input pulse, but the duration is thousands of times longer. This makes it possible to measure the profile of ultrashort optical pulses (< 1 ps) with currently available and relatively slow photodetectors and other electronic test equipment. The measurement is performed directly in the time-domain and does not involve any manipulation in the frequency-domain. It is also done in a single shot and there is no mechanical movement

involved. This not only reduces the system complexity, but also avoids errors caused by non-identical pulse shapes in a pulse series. It can be expected that the temporal microscope will soon have substantial impact on the ultrafast optoelectronics community.

2.4.2 Optical pulse shape restoration by temporal filtering

Optical fiber communication technology plays a critically important role in the implementation of information superhighways. In an optical fiber communication system, information is encoded into a series of optical pulses and transmitted through optical (single mode or multimode) fibers. The high bandwidth of optical fiber offers a tremendous data capacity. However, due to the group velocity dispersion, the shape of optical pulses is distorted, or blurred, after traveling through a certain distance. As an example, a nearly rectangular optical pulse may become a bell-like and expanded pulse. Consequently, the leading edge of a second pulse may catch up the tailing edge of the first pulse and, therefore, cause cross talk.

To overcome this problem, a repeater must be deployed before the distortion in pulse shape gets too bad to recover. In a repeater, the optical signal is detected by a photodetector. The detected electronic signal is then amplified, reshaped, and fed to a light source, such as a light emitting diode or a laser diode. Because of the optic-to-electronic and electronic-to-optic conversions, the huge bandwidth of optics cannot be fully utilized in today's fiber communication systems. Recently, optical amplifiers have been developed that make it possible to amplify the attenuated optical signal directly. Nevertheless, the optical signal still needs to be converted into an electronic signal in order to restore the shape of the blurred optical pulses.

The 4-f temporal filtering system offer the possibility to eliminate the requirements of optic-to-electronic and electronic-to-optic conversions. Since the dispersion behavior of an optical fiber can be accurately characterized, an inverse filter can be designed that cancels the blur in pulse shape caused by group velocity dispersion. Assume the original optical pulse is expressed by $s(\tau)$ and the dispersion property of the optical fiber is characterized by $d(\tau)$, the output pulse at the end of the optical fiber can be written as

$$o(\tau) = s(\tau) \otimes d(\tau) \qquad (57)$$

where $\otimes$ denotes the convolution operator. Such output pulses are fed into the 4-f temporal filter system depicted in Fig.7. The inverse filter is of the form

$$F(\Delta f) = \frac{1}{D(\Delta f)} \qquad (58)$$

where $D(\Delta f)$ is the Fourier transform of $d(\tau)$. After passing through the 4-f system, the original shape of the optical pulse is restored:

$$r(\tau) = F^{-1}\{S(\Delta f) \cdot D(\Delta f) \cdot F(\Delta f)\} = s(\tau) \qquad (59)$$

Since the operation of the 4-f temporal filtering system is performed fully optically, no electronic-to-optic and optic-to-electronic conversions are needed. This will lead to more efficient use of the huge bandwidth provided by optical fibers and, therefore, a boom in data capacity of optical fiber

communication systems.

2.5 Preliminary Design of Deliverable Prototype

The temporal imaging and possessing systems identified for Phase II prototype development are the temporal microscope shown in Fig.6 and the temporal 4-f filtering system shown in Fig.7. The targeted applications of these two systems are picosecond optical pulse shape measurement and optical pulse shape deblurring in fiber communication networks.

For convenience of alignment and testing, the operation wavelength is chosen to be 670 nm, at the red end of the visible range. Diode lasers with either internal or external modulations can be used as light sources. The modulation circuits for the diode lasers are planned to be developed by Quantex personnel. The output can be detected by high-speed photodetector or evaluated with optical correlators. The system components and their providers, specifications, and cost are listed in Table.5.1.

All the parameters for the components were determined based on the products commercially available at the present time. The construction of the prototype systems can be started immediately when Phase II support becomes available.

Table 5.1 Component list for prototype development

Item	Provider	Specifications	Unit Price
Laser Diode	LaserMax LAS-200-670-10	670 nm, 10 MW Single Spatial Mode	$650
LD modulator	Quantex Built In-House	Subnenosecond Pulse Generation	$4,000
EO Modulator	New Focus Model 4841	BW: 3 - 10 GHz A=32 @ 670 nm P < 5 W, $LiTaO_3$	$5,250
EOM Driver	New Focus Model 3211	Gain: 40 V/V DC Offset: ±200 V	$2,950
Grating	Spectrogon	500 - 3000 lp/mm Size: 110x110 mm^2	about $1,500
Photodetector	New Focus Model 1002	DC to 60 GHz 6 ps rise time 400-900 nm	$6,000

3. CONCLUSIONS

The concept of time lens is based on the analogy between optical spatial diffraction and temporal dispersion. It extends our knowledge of optics in the space-domain into the time-domain. Novel temporal imaging and signal processing systems can be created that mimic the operation of their spatial counterparts in the space-domain. The objective of the Phase I work was to determine the technical feasibility and design time lenses with off-the-shelf devices.

This objective has been successfully achieved. During the Phase I period, we studied the space-time duality and established a theoretical model for general temporal imaging systems. Design criteria for a phase chirp modulator as well as dispersive delay lines have been developed. Several temporal imaging and signal processing systems have been designed with commercially available optic and optoelectronic devices. Various applications of these temporal processing systems were studied. A temporal microscope and a temporal 4-f filtering system have been identified for prototype development in Phase II.

4. RECOMMENDATIONS FOR PHASE II WORK

The following tasks are suggested for the Phase II work:

1. Theoretical study of space-time duality and temporal imaging system design techniques

   A more thorough study on space-time duality and temporal imaging concept will be conducted. The possibility of introducing the well developed spatial imaging system design techniques, such as Collins chart, ABCD matrix, and operator algebra, etc., into the design of temporal imaging systems will be investigated. The aberration in an temporal imaging system will be studied.

2. Application investigation of temporal imaging and processing systems

   Various applications, military or commercial, of time lens based temporal imaging and/or signal processing systems will be explored. Emphases will be placed on the applications where the ultrafast, all-optic operations are exclusively needed. Novel concepts and architectures can be envisioned as the results of such exploration.

3. Construction and evaluation of prototype systems

   A prototype telecentric temporal microscope and a prototype temporal 4-f filtering system will be constructed with off-the-shelf devices. The applications of these prototypes include, but are not limited to, picosecond optical pulse shape measurement and optical pulse shape deblurring in fiber communication networks. The developed prototype systems will be experimentally characterized and evaluated.

4. Delivery of the prototype systems

The developed prototype systems will be delivered to the contract sponsor by the end of the Phase II program. A detailed manual including optical system arrangement, specification of all components, system alignment requirements and procedures, operation instructions, troubleshooting and maintainence, etc., will be provided upon the delivery of the prototypes.

5. REFERENCES

[1]. H. J. Caulfield and G. Gheen, eds., *Optical computing* (SPIE press, Bellingham, 1989).

[2]. F. T. S. Yu and S. Yin, eds, *Coherent optical processing* (SPIE press, Bellingham, 1993).

[3]. J. Schamir, "Fundamental speed limitations on parallel processing," Appl. Opt., **26**, 1507(1987).

[4] A. W. Lohmann and A. S. Marathay, "Globality and speed of optical parallel processors," Appl. Opt., **28**, 3838(1989).

[5]. J. N. Lee, A. Husain and J. Crow, *Special issue on optical interconnections for information processing*, J. Lightwave Tech., **9**, 1633(1991).

[6]. A. Bjaklev, *Optical fiber amplifiers: design and system applications*, (Artech House, New York, 1993).

[7]. S. A. Akhmanov, A. S. Chirkin, K. N. Drabovich, A. I. Kovrigin, R. V. Khokhlov and A. P. Sukhorukov, "Nonstationary nonlinear optical effects and ultrashort light pulse formation," IEEE J. Quantum Electron., **QE-4**, 598(1968).

[8]. D. Grischkowshy and A. C. Balant, "Optical pulse compression based on enhanced frequency chirping," Appl. Phys. Lett., **41**, 1(1982).

[9]. D. Grischkowshy, "Optical pulse compression," Appl. Phys. Lett., **25**, 566(1974).

[10]. B. H. Kolner, "Active pulse compression using an integrated electro-optic phase modulator," Appl. Phys. Lett., **52**, 1122(1988).

[11]. J. W. Goodman, *Introduction to Fourier optics* (McGraw-Hill, New York, 1968).

[12]. B. H. Kolner and M. Nazarathy, "Temporal imaging with a time lens," Opt. Lett., **14**, 630 (1989).

[13]. M. Born and E. Wolf, *Principle of optics, sixth edition*, (Pergamon, Oxford, 1970).

[14]. H. A. Haus, *Waves and fields in optoelectronics* (Prentics-Hall, Englewood Cliffs, 1984).

[15]. G. P. Agrawal, *Nonlinear fiber optics* (Academic, New York, 1989).

[16]. New Focus, Product catalog (New Focus Inc, Mountain View, 1993).

[17]. E. B. Treacy, "Optical pulse compression with diffraction gratings," IEEE J. Quantum Electron., **QE-5**, 454(1969).

[18]. A. W. Lohmann and D. Mendlovic, "Temporal filtering with time lenses," Appl. Opt., **31**, 6212(1992).

[19]. T. Yajima et al, eds., *Ultrafast phenomena VI* (Springer-Verlager, Berlin, 1988).

[20]. W. Sibbett, "Synchroscan streak camera system," Proc. SPIE, **348**, (1982).

[21] A. Yarif, *Optical Electronics*, 4th edition, pp.200-204(HRW Sounders, Philadelphia, 1991)

[22] J.-C. M. Diels, J. J. Fontaine, I. C. McMichael and F. Simoni, "Control and measurement of ultrashort pulse shapes with femtosecond accuracy," Appl Opt., **24**, 1270(1985).

[23] J. E. Rothenberg and D. Grischkowsky, "Measurement of optical phase with

subpicosecond resolution by time-domain interferometry,"
[24] J. Janszky, G. Corradi and D. S. Hamilton, "Temporal analysis of short laser pulses using degenerated four wave mixing," Appl.Opt., **23**, 8(1984).
[25] Y. R. Shen, *The Principles of Nonlinear Optics*, (Wiley, New York, 1984).
[26] N. G. Paulter and A. K. Majumdar, "A new triple correlation technique for measuring ultrashort laser pulses," Rev.Sci.Instrum. **62**, 567(1991).
[27] N. G. Paulter and A. K. Majumdar, "A new triple correlator design for the measurement of ultrashort laser pulses," Opt.Commun. **81**, 95(1991).